DOI 10.1007/s10812-019-00839-9
Journal of Applied Spectroscopy, Vol. 86, No. 3, July, 2019 (Russian Original Vol. 86, No. 3, May–June, 2019)

DYNAMIC RANGE OF CCD PHOTOSENSORS FOR ATOMIC-EMISSION ANALYZERS

A. D. Yegorov, V. A. Yegorov,* and S. A. Yegorov UDC 543.423

The dynamic range of charge coupled devices (CCD) is studied by an example of type TCD1304AP detectors in atomic-emission spectrometers. For this we have used an instrument developed by us with original methods for measuring the sensor temperature and analyzing nonlinear distortions at different signal levels. The principle of reciprocity of spectrum line brightness and exposure is used to monitor the nonlinearities of the paths for charge accumulation and transfer. The processing of measurement data and compensation of nonlinear distortions at different signal levels were carried out using a maximum likelihood method. Conditions were identified under which distortions arise at low, as well as high signal levels. A method for extending the dynamic range of CCD detectors based on the blooming effect is proposed.

Keywords: *atomic-emission analysis, charge coupled devices, reciprocity law, maximum likelihood method, recording of spectra, dynamic range.*

Introduction. Experimental studies of CCD detectors, which are widely used in atomic-emission spectrometers, indicate that their dynamic range is insufficient for solving some problems in elemental analysis by plasma spectroscopy [1–3]. It is known that a heated substance in the gaseous state emits a line spectrum in which the intensity of a line radiated by an excited atom during an electronic transition from level m to the ground state is given by [4]

$$I(T) = B \exp(-E_m/RT), \quad (1)$$

where B is a constant, E_m is the energy of the excited level, R is the universal gas constant, and T is the absolute temperature of the material. According to Eq. (1) the influence of the plasma temperature on the line intensity is especially strong, since the temperature shows up in the exponent. The plasma formations used in atomic-emission spectrometry are usually spatially inhomogeneous and temporally transient; this imposes specific requirements on the dynamic range of the radiation detector.

The dynamic range of CCD and CMOS detectors has been determined [5] for the case of uniform levels of illumination of all the pixels by a powerful source. A similar approach has been used [6] for analyzing the dynamic range of light-emitting diodes. The dynamic range of detectors for detection of powerful sources emitting over a comparatively broad range was studied in [5–6]. The methods used there did not account for all the specifics of narrow-band atomic-emission spectra. The determination of the position and amplitude of spectrum lines during operation of a detector in the linear segment of the light signal characteristic was discussed in [7–10], but summation of readings from several pixels near the spectral peak is not the optimum way of processing the measurement data. This kind of processing using the *rect*-function as the smoothing kernel does not take the shape of the apparatus function of the spectrometer into account, as noted in [11]. It has been shown [11] that, in order to determine the amplitude of a spectrum line using the *rect*-function, it is necessary to know the position of its maximum relative to the pixels of the photodetector array with high accuracy. A more correct approach to determining the position and amplitude of spectrum lines employing a least squares method is used in [12].

The Effect of Dark Current on the Dynamic Range of a Detector. We consider the problem in a general spectrometric formulation. Let the distribution of the power in a spectrum line for a light signal $f(\lambda)$ appear in the focal plane of a spectrograph in the form of a dependence $f(x)$, where the coordinate x is directed along the dispersion of the instrument.

*To whom correspondence should be addressed.

O. Ya. Usikov Institute of Radiophysics and Electronics, National Academy of Sciences of Ukraine, 12 Akademika Proskury Str., Kharkiv, 61085, Ukraine; email: yegorov@ire.kharkov.ua. Translated from Zhurnal Prikladnoi Spektroskopii, Vol. 86, No. 3, pp. 410–416, May–June, 2019. Original article submitted November 30, 2018.

The quantity $f(x)$ is converted by a multielement photoelectric detector into a one-dimensional sequence of readings of an electrical signal f_n which is the result of integrating the function $f(x)$ over the area of pixel number n during the exposure time.

$$f_n = \tau \left[\theta_n(T) + Q_n \int_{x_n}^{x_{n+1}} f(x + \varphi) dx \right] + N_n \ , \qquad (2)$$

where τ is the exposure time, T is the crystal temperature, $\theta_n(T)$ is the dark current as a function of temperature, Q_n is the light-signal characteristic of the nth pixel of the photodiode array, and N_n is the noise component, and φ is an instrument parameter characterizing the position of the image of the spectrum relative to the detector array (which can be varied deliberately during scanning of the spectrum, as is done for subpixel resolution of the detector [14], or randomly owing to thermal and mechanical interactions). The noise component N_n contains readout noise, digitization noise from the analog-to-digital converter (ADC), and several other components.

We shall examine problems associated with the dark current $\theta_n(T)$. It is known that the dark current of a detector changes by a factor of two for every 7°C change in the crystal temperature [15]. As one of the terms in a single measurement, the dark current occupies part of the dynamic range of the detector. For high temperatures and long exposures, the contribution of this term can lead to off-scale readings of the detector. Thus, for operation under actual conditions of a factory laboratory or production line, it is desirable to cool the detectors or at least monitor their temperature. Separate sensors that measure the temperature of an electrical circuit or the whole spectrometer are customarily used to measure the temperature and these data are the basis for the use of Peltier cells to thermally stabilize the system [8–10].

Measurement of the temperature of the crystal of each chip makes the scheme more complicated and leads to some design problems. To reduce the complexity we have studied the feasibility of determining the crystal temperature using characteristics of the measured signal to solve the problem at a program level.

The Experimental Setup is a measurement system consisting of a plasma source, a DFS-452 spectrograph, and a photoelectric detector unit. A specialized computer program is used for system operation and data processing. The photoelectric circuit described in [16] is used instead of a photoelectric plate in the spectrograph. It is supplemented with means for measuring and controlling the temperature of the photodetector crystal from –20 to +40°C. The temperature was controlled with a temperature controller based on Peltier cells and semiconductor temperature sensors. The controller was calibrated at the beginning and end of the measurements. In addition, the apparatus includes a circuit for synchronization and control, an ADC, and interfaces for connection to the base computer. TCD1304AP linear CCD sensor arrays (Toshiba) were used for detecting the light flux.

The dark currents were analyzed at temperatures from –20 to +30°C and for exposure times of 0.035 to 4 s. The measurement data were used to study the accuracy of the temperature determination with respect to several of the dark current parameters that were studied. The greatest accuracy was obtained when the parameter was the difference between the digitized signal without illumination and the instrument zero measured after completion of the readout of the active pixels from the shift register of the CCD. The mean square error in the temperature measurement was ~0.1°C. The permissible range of operating temperatures and exposure times for photometry of spectra was found by analyzing the detector dark current.

In spectral analysis practice, the effect of dark current is often minimized by simply subtracting it from the measurement data [17]. To do this the optical input of the spectrometer is blocked before or after a spectrum is taken and the dark current is recorded with the accompanying noise and pickup. The difference between these two traces does not contain the constant component of the dark current. This difference determines the lower limit of the working segment of the light-signal transfer function of the sensor. The ratio of the maximum and minimum values of the working characteristic determines the dynamic range of the sensor. In order to estimate this ratio it is necessary to know the degree of nonlinearity of the transfer function over the limits of the entire working characteristic.

A Study of the Nonlinearity of the Light-Signal Transfer Function of a Sensor. The dependence of the transfer function of the sensor on exposure time is studied by plotting the variation in the profiles of spectrum lines with different brightnesses with the dark current subtracted. Photometry of an isolated line obtained with eight exposures from 0.1 to 4 s (Fig. 1) shows that an acceptable level of distortion was obtained only with the three shortest exposures. In the other cases the signal is burdened with significant nonlinear distortions; it is bounded above and has a highly extended trailing edge. This is related to the features of the accumulation and readout of charge in CCDs. The circuits for accumulation, transfer, and transport of charge are overfilled, so charge is lost and flows into neighboring cells (the blooming effect). Features of accumulation and readout in the detector also lead to significant waviness in the saturation at the maximum signal levels.

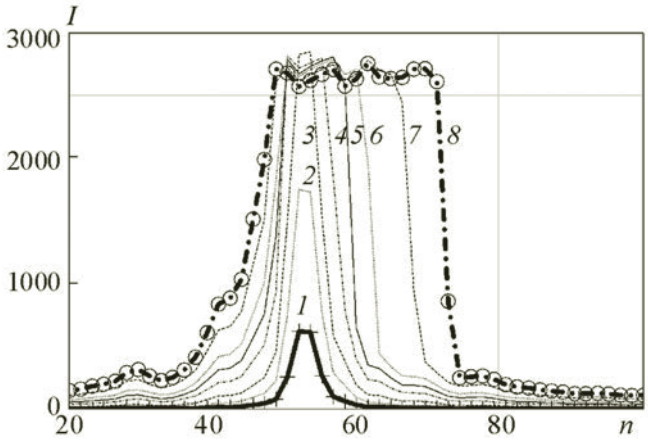

Fig. 1. Results of photometry of a mercury spectrum line $I(n)$ with exposure times of 0.10 (1), 0.25 (2), 0.50 (3), 1.00 (4), 1.50 (5), 2 (6), 3 (7) and 4 s (8).

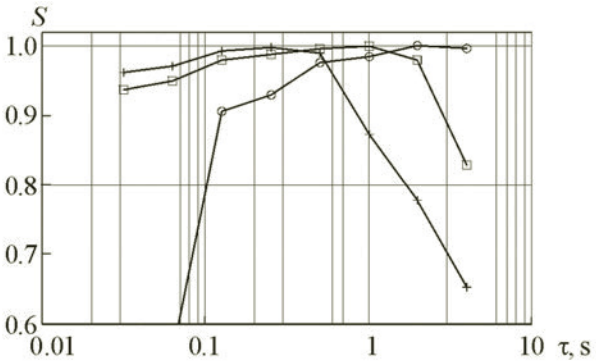

Fig. 2. The areas under plots of the distribution of brightness $S(\tau)$ as a function of exposure for spectrum lines with amplitudes of 11 (○), 115 (□), and 560 arbitrary units (+).

These shortcomings make it impossible to separate close lying lines and makes the analysis of isolated lines more difficult. In the example of Fig. 1, only the first three exposures are adequate for measurements if the amplitude of a spectrum line is chosen as the analytic parameter. Instrumental and program means can be used to fight blooming.

Of the instrumental means for fighting the spreading of charge, the best is the use of CCD detectors with anti-blooming or detectors fabricated with other technologies that are not subject to blooming. They also have light-signal characteristics with nonlinearities that can be countered to a greater or lesser extent by the methods discussed here. They are, however, significantly more expensive that the Toshiba TCD1304AP CCD detectors discussed above. The instrumental means include attempts to reduce the readout noise by changing the shape and duration of the array control pulses, but the maximum gain from this is only 10%.

Of the programming techniques, we should note an optimal choice of exposure as a function of the brightness and shape of the spectrum line being analyzed, as well as a correct choice of the analytic parameter [18]. Let us consider the use of the area under the distribution curve of a spectrum line as the analytic parameter, rather than the amplitude of the line. The behavior of this parameter with exposure duration depends on the principle of reciprocity of brightness and exposure. This principle is known in photochemistry as the Bunsen–Roscoe law and in photographic photometry as the Schwarzschild law. When it is satisfied in the present case, the product of the area under the brightness distribution curve in the line and the exposure duration should not depend on the exposure. For a linear light-signal characteristic this product should be the same for all exposures.

If we plot these values as a function of exposure, then when the principle of reciprocity is satisfied, a horizontal straight line should result, as in [7]. In fact, the line is never straight or horizontal. If the data obtained in this way are

normalized for each spectrum line with respect to its maximum magnitude, then this yields the dependence of area on exposure $S(\tau)$ shown in Fig. 2. The photometric data for three spectrum lines with intensities in a proportion of ~11:115:560 imply that the reciprocity principle obtained in this way can be violated at both minimal and maximal exposures.

We cannot but agree with Kostrin [3] in that, based on physical considerations, at low signals this law should not be violated. Nevertheless, under certain circumstances it fails, in both [3] and the present paper. This is because, as the exposure is reduced the amount of accumulated signal approaches zero and may become comparable to the noise. Then subtraction of the dark current may yield a sign-changing value. The average of this difference as the exposure decreases will approach zero, which is observed experimentally. Naturally, when the line is fainter this effect shows up more strongly (Fig. 2). In analytic practice, a background is typically present so this effect can be neglected. In addition, the influence of these factors can be reduced by more correct processing, e.g., using a least squares method. To do this, additional parameters which exclude the appearance of negative intensity values need to be introduced. Low intensity spectrum lines only experience amplitude distortions; unlike strong lines, their shape does not change. For high signals, as Fig. 1 implies, the shape of the spectrum lines is distorted so much that it becomes difficult to approximate them analytically. Thus, we propose including these features of the apparatus function in a generalized parameter which is determined experimentally in the form of a table.

Linearizing the Light-Signal Transfer Function of a CCD Detector for Large Signals. Since the amplitudes of a large number of analyzed lines and comparison lines differ, it is necessary to have a suitable dynamic range for undistorted simultaneous photometry of these lines. If this cannot be done, then a linearization procedure employing data on fits to the reciprocity principle similar to Fig. 2 is invoked. An analogous procedure is followed when antiblooming sensors are used [19]. Antiblooming always assumes that they have a nonlinear light-signal characteristic owing to charge leakage in excess of a certain value. But every type of loss, including that of charge, has a negative effect on accuracy. In this sense CCD detectors without antiblooming make a more complete record of the charge generated by the light, although this leads to broadening and asymmetric deformation of the spectrum lines. Spreading of charge to one side is especially harmful, as this masks neighboring lines. This effect was studied by simultaneously recording a spectrum on two strips separated by 180^{o}. The resulting photometry of a very bright line is shown in Figs. 3a and b, which shows the same line for two exposure times with charge transport in opposite directions. If they are mentally cut symmetrically relative to the spectrum line recorded on the linear segment of the light-signal characteristic (curve 2) and then folded along the cut line, then the single plot shown in Fig. 3c can be constructed from the two plots.

If least squares methods are used to complete this procedure, then it should be sufficiently correct. The "cut" part is best used for estimating the amplitude parameter. Thus, for estimating the area under the spectrum line, the existence of blooming can change from a shortcoming to an advantage. As a result, we obtain linearly recorded faint lines and recovered sparse strong lines. The amplitude characteristics of these strong lines can be recovered by invoking data on their broadening (Fig. 1) and on satisfaction of the principle of reciprocity (Fig. 2), so that the dynamic range can sometimes be increased. The degree of possible broadening depends on the shape of the spectrum, and a more reliable conclusion regarding the applicability of this method can only be obtained on the basis of the results of its practical application. For example, according to the data of Fig. 3 the spectrum line is broadened by a factor of ~16 owing to blooming and one can hope for a similar increase in the dynamic range. In reality, it is somewhat less because of losses associated with breakdown of the reciprocity principle which, judging from Fig. 2, may extend to 40%. In the concrete case of Fig. 3a and b, the ratio of the areas under lines 1 and 2 is ~14.7. Thus, these transformations yield a linearized version of the spectrum with an increased dynamic range. For final processing of the linear version it is best of all to use a maximum likelihood method [12].

Let the apparatus function $f(x, p_\alpha)$ of the spectrometer depend on the coordinate x and a number of parameters p_α, where α denotes the order number of a parameter. The spectrum is recorded in n measurements at points x_i $(1 \le i \le n)$ with mean square errors ε_i. These data yield a sequence of n readings:

$$f_i = f(x_i, p_\alpha) + \varepsilon_i \,. \tag{3}$$

In accordance with the approach of [12], we find the most probable values of the parameters by minimizing the sum of the squares of the deviations between the *a priori* data and the measurements. In this case, the logarithmic likelihood function has the form

$$L(x,\ p_\alpha) = \text{const} - \frac{1}{2\sigma^2} \sum_{i=1}^{n} \left[f(x_i,\ p_\alpha) - f_i \right]^2 , \tag{4}$$

where σ^2 is the normal noise power.

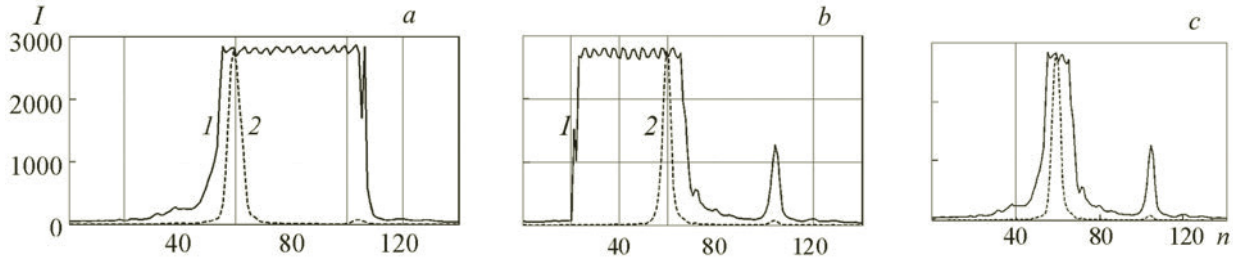

Fig. 3. Spectra with an exposure of 4 s, with charge spread (1) and with an exposure of 0.25 s under conditions close to a linear regime (2), with rightward (a) and leftward (b) shifts in the transport register; (c) a spectrum with a long exposure compiled from undistorted parts of a strongly overilluminated line (smooth curve) and the same line with a short exposure (dotted curve).

To determine the set of parameters that minimize Eq. (4), we set the partial derivatives of the likelihood functions with respect to all the parameters equal to zero:

$$\sum_{i=1}^{n} \left[f(x_i,\ p_\alpha) - f_i \right] \frac{\partial f(x_i,\ p_\alpha)}{\partial p_\alpha} = 0\,. \tag{5}$$

As a result, we obtain a system of equations with respect to the unknown parameters. The solution of this system yields a set of their most probable values $\overline{p}_\alpha$.

The characteristic error is the second derivative of the likelihood function with respect to the corresponding parameter for $p_\alpha = \overline{p}_\alpha$:

$$\frac{\partial^2 L}{\partial p_\alpha^2} = \sum_{i=1}^{n} \left[\frac{\partial f(x_i,\ p_\alpha)}{\partial p_\alpha} \right]^2 . \tag{6}$$

For measurements of the signal amplitude in the case of a linear detector transfer characteristic, the apparatus function of the spectrometer can be written in the form

$$f(x, p_\alpha) = Av(x)\,, \tag{7}$$

where A is the unknown amplitude characteristic of the spectrum line and $v(x)$ is a function describing the distribution of the brightness of the spectrum line along the dispersion normalized with respect to the maximum or integral of the function. If the linear region of the detector is not exceeded, then $v(x)$ is independent of the amplitude and Eq. (5) can be written in the form

$$\sum_{i=1}^{n} \left[f(x_i,\ A) - f_i \right] v(x_i) = 0\,. \tag{8}$$

On substituting Eq. (7) in Eq. (8), to within a constant we obtain

$$A = \textstyle\sum_i f_i v(x_i)\,, \tag{9}$$

which describes the procedure for smoothing the experimental data by a stationary kernel $v(x)$ in terms of the maximum likelihood method. The smoothing kernel $v(x)$ is often taken to be the function rect(x) (when summing over a certain number of pixels [8, 10, 17] or using a Gaussian normal distribution function [18]). It is intuitively understandable that using a rectangular smoothing kernel is not optimal for several reasons. In this case, all readings of a spectrum line are averaged with the same weight, although the signal-to-noise ratio is higher near its maximum than at the edges. The result also depends on the width of the smoothing window and its position relative to the detector array. When the window is widened, the accuracy increases but the resolution is reduced. Thus, it is sometimes necessary to turn to manual control involving an operator, which increases the subjective component of the error. This point is also discussed in [11]. For these reasons, it is preferable to use the above discussed maximum likelihood method when analyzing the measurement results. This is confirmed by one

of the major properties of this method: if a sufficient and effective estimate for the parameter exists, then this method yields precisely this estimate and a more precise estimate cannot be found [20].

Conclusions. An analysis of the experimental results shown here yields the following conclusions. Subtraction of the dark current and other noise components recorded at the closed input of a spectrograph can lead to distortion of the measurement results for short exposures. In this case, the resulting difference may change in sign and the reciprocity principle may be violated; this leads to amplitude distortions in the detection of faint light fluxes and requires corresponding corrections in the analysis algorithms. When a background greater than the dark current is present, subtraction does not lead to negative intensities and this factor is usually ignored. The major limiting factor in the dynamic range for high signals is overload of the acquisition and transfer circuits by the detector structures (blooming). This harmful effect can be used to extend the dynamic range of a photodetector.

When the influence of these factors on the results of an analysis is reduced, it is proposed that the nonlinearities in the charge acquisition and transfer circuits be monitored with respect to the reciprocity principle and exposure duration. This principle is a very sensitive indicator in the case of weak signals, as well as during overload. When weak signals are being detected, careful monitoring of the temperature of the detector crystal is needed. For determining the crystal temperature under actual operating conditions it is appropriate to use the excess of the dark current level above the instrumental zero. Tests show that the proposed method provides an accuracy of better than 0.1^{o}C for positive temperatures and can be performed on a program level, rather than instrumental, with preliminary calibration during preparation of the apparatus. In the case of large signals it is necessary to choose the analytic parameters that are least subject to overload effects. Our estimates show that the area under a spectrum line is the most suitable amplitude parameter. A method for using charge that expands asymmetrically during overload has been proposed for extending the dynamic range with mutually oppositely directed CCD transport arrays for the spectrum. This involves a doubling of the number of detectors, but makes possible a manifold increase in the dynamic range.

REFERENCES

1. Jian-Kang Zhou, Wei-Min Shen, and Min-Xue Tang, *Opto-Electron. Eng. J.*, **33**(10), 96–114 (2006).
2. A. A. Ukhov, *Optical Spectrometers with Multielement Photodetectors*, Author's Abstract, Dr. of Tech. Sciences, LÉTI, St. Petersburg (2015).
3. D. K. Kostrin, *Izv. SPbGÉTU*, No. 1, 6–7 (2015).
4. A. A. Pupyshev, Atomic-absorption Spectral Analysis [in Russian], Tekhnosfera, Moscow (2009).
5. D. T. McCormick, *Line Array Sensor Comparison*, Hamamatsu S11639, Sony ILX511B, Toshiba TCD1205DG; http://www.advancedmems.com/pdf/AMEMS_LineSensorArraySummary_v1.pdf.
6. R. V. Yudin, D. K. Kostrin, D. E. Shipov, and A. A. Ukhov, *Izv. SPbGÉTU*, No. 3, 8–13 (2013).
7. D. K. Kostrin, A. A. Lisenkov, A. A. Uhov, and A. N. Ramazanov, *J. Phys*., *Ser. Conf*., **729**, 012030 (2016).
8. Ya. I. Didkovskii, M. N. Kovalenko, A. A. Min'ko, and M. R. Posledovich, *Vestn. BGU*, Ser. 1, No. 1, 21–25 (2015).
9. V. A. Labusov, V. G. Garanin, and I. R. Shelpakova, *Zh. Analit. Khim*., **67**, No. 7, 697–707 (2012).
10. A. D. Demin and Yu. P. Chugunov, *Opt. Zh*., **79**, No. 3, 51–55 (2012).
11. A. D. Yegorov, V. A. Yegorov, S. A. Yegorov, and E. V. Zdor, *Radiofiz. Élektronika*, **7**, No. 2, 422–425 (2002).
12. E. L. Kosarev, *Methods for Processing Experimental Data* [in Russian], Fizmatlit, Moscow (2008).
13. A. D. Yegorov, V. A. Yegorov, S. A. Yegorov, L. I. Elenskaya, and I. E. Sinel'nikov, *Vesti NTUU "KPI," Ser. Priborostroenie*, **48**, No. 2, 74–80 (2014).
14. A. Yegorov, V. Yegorov, and S. Yegorov, *Radiofiz. Radioastronomiya*, **14**, No. 1, 77–83 (2009).
15. M. Howes and D. Morgan (Eds.), *Charge Coupled Devices* [Russian translation], Energoatomizdat, Moscow (1981).
16. V. A. Yegorov and S. A. Yegorov, *Nauka Iinnovatsiya* (Kiev), **4**, No. 2, 33–39 (2008).
17. V. G. Garanin, O. A. Neklyudov, D. V. Petrochenko, Z. V. Semenov, I. G. Shatalov, and S. V. Pankratov, *Zav. Lab. Diagnostika Materialov*, **78**, No. 1, Part II, 69–74 (2012).
18. I. E. Vasil'eva, A. M. Kuznetsov, I. L. Vasil'ev, and E. V. Shabanova, *Zh. Analit. Khim*., **52**, No. 12, 1238–1248 (1997).
19. Jianping Tong, Jianxun Gao, Fei Wang, and Hao Yang, *Opto-Electron. Eng. J*., **44**, No. 11, 1101–1106 (2017).
20. D. Hudson, *Statistics for Physicists* [Russian translation], Mir, Moscow (1970).